Thermoplastic, rubber-like marine antifouling coatings with micro-structures via mechanical embossing

Biofouling
The Journal of Bioadhesion and Biofilm Research

ISSN: 0892-7014 (Print) 1029-2454 (Online) Journal homepage: https://www.tandfonline.com/loi/gbif20

Thermoplastic, rubber-like marine antifouling coatings with micro-structures *via* mechanical embossing

Tom Bus, Marie L. Dale, Kevin J. Reynolds & Cees W. M. Bastiaansen

To cite this article: Tom Bus, Marie L. Dale, Kevin J. Reynolds & Cees W. M. Bastiaansen (2020) Thermoplastic, rubber-like marine antifouling coatings with micro-structures *via* mechanical embossing, Biofouling, 36:2, 138-145, DOI: 10.1080/08927014.2020.1734576

To link to this article: https://doi.org/10.1080/08927014.2020.1734576

BIOFOULING
2020, VOL. 36, NO. 2, 138–145
https://doi.org/10.1080/08927014.2020.1734576

Taylor & Francis
Taylor & Francis Group

Thermoplastic, rubber-like marine antifouling coatings with micro-structures *via* mechanical embossing

Tom Bus[a], Marie L. Dale[b], Kevin J. Reynolds[b] and Cees W. M. Bastiaansen[a,c]

[a]Laboratory of Stimuli-Responsive Functional Materials & Devices, Department of Chemical Engineering and Chemistry, Eindhoven University of Technology, Eindhoven, The Netherlands; [b]AkzoNobel/International Paint Ltd, Gateshead, UK; [c]School of Engineering and Materials Science, Queen Mary University of London, London, UK

ABSTRACT

New processing routes and materials for non-biocidal, antifouling (AF) coatings with an improved performance are currently much sought after for a range of marine applications. Here, the processing, physical properties and marine AF performance of a fluorinated coating based on a thermoplastic (non-crosslinked) fluorinated polymer are reported. It was found that the addition of lubricating oil and hydrodynamic drag reducing microstructures improved the AF properties substantially, i.e. the settlement of a marine biofilm, containing mixed microalgae including diatoms, was reduced to low levels. More importantly, the remaining fouling was removed from the coatings at low hydrodynamic shear rates and promising AF properties were obtained. Moreover, additional potential benefits were revealed originating from the thermoplastic nature of the coating material which might result in significant cost reductions.

ARTICLE HISTORY
Received 22 July 2019
Accepted 19 February 2020

KEYWORDS
Thermoplastic fluoropolymers; surface topography; biofilm assays; foul-release; marine coatings

Introduction

The accumulation of biological organisms on surfaces, referred to as biofouling, is a widespread problem with impacts in multiple sectors (Schultz 2007; Harding and Reynolds 2014; Deshpande et al. 2015; Jiang et al. 2017). Marine biofouling has a substantial economic impact and, for instance, increases fuel consumption and costs for the shipping industry (Schultz 2007; Schultz et al. 2011). Conventional coatings for marine anti-biofouling are based on biocidal technologies and their use results in extensive release of toxic and bio-accumulative compounds into the marine environment and eventually the food chain (Konstantinou and Albanis 2004; Thomas and Brooks 2010; Dafforn et al. 2011). There is therefore a need for novel, effective and non-toxic coatings to replace biocidal antifouling (AF) coatings (Lejars et al. 2012; Nurioglu et al. 2015).

Recently, oil-infused crosslinked polymers have shown promise in this regard (Boggs et al. 2012; Xiao et al. 2013; Miserez et al. 2017; Kommeren et al. 2019). In these systems, crosslinked synthetic polymers based on fluoropolymers or polydimethylsiloxanes (PDMS) are used with a large volume fraction of oligomeric species, lubricants and/or oils. A thin liquid layer is generated on the material surface and the lubricant diffuses from the coating to the water interface and this liquid layer is replenished as it becomes depleted. These coatings are capable of repelling a range of contaminants including ice, blood, and bacteria, and have proven highly effective in resisting bacterial adhesion under both static and flow conditions (Wong et al. 2011; Xiao et al. 2013; Yao et al. 2014; He et al. 2018).

The ability to further tailor AF properties with surface relief structures in lubricant infused coatings potentially further expands the functionality and applications of these coatings. For example, the implementation of surface relief structures in crosslinked fluoropolymers increases control over wettability and influences cellular adhesion in application areas such as AF coatings (Yao et al. 2014). These surfaces have the capability to repel a wide variety of liquids, including water, hydrocarbons, crude oil or blood, using a combination of surface topographies.

Despite the enormous progress in the field of non-toxic AF coatings it is still challenging to create new low cost materials and processing routes that

CONTACT Cees W. M. Bastiaansen C.W.M.Bastiaansen@tue.nl
This article has been republished with minor changes. These changes do not impact the academic content of the article.

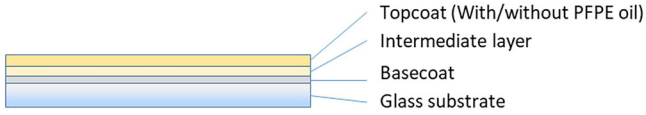

Figure 1. Schematic representation of the coating scheme used for micro-structuring with drag reducing micro-structures and antifouling testing.

allow tailoring of the AF properties for improved performance. As a proof of concept, a new fluorinated, non-biocidal and non-crosslinked polymer containing a lubricant was investigated with a special emphasis on coatings containing hydrodynamic drag reducing structures. The thermoplastic nature of these coatings reduces materials and processing cost which might be an important feature for their widespread use. More importantly, it is shown that these thermoplastic coatings have a low settlement of marine biofilm (comprising of mixed microalgae, including diatoms) and that the marine biofilm is easily removed at low hydrodynamic shear rates. These excellent AF properties combined with stable microstructures *via* a simple embossing process make it beneficial in, for instance, shipping applications.

Materials and methods

Materials

A thermoplastic elastomer (TPE) was used (polyvinylidenefluoride hexafluoropropylene (P(VDF-HFP), Tecnoflon® N215) which was supplied by Solvay SA and which is referred to by the supplier as a fluoroelastomer copolymer. The TPE was tested *via* multiple techniques (XRMA, GC-MS, GPC and NMR) for toxic species and these were not found. The lubricant, a perfluorinated polyether (PFPE, Fluorolink E10/6) was also kindly supplied by Solvay SA. A perfluorinated copolymer (fluorinated ethylene propylene copolymer (FEP, TEFLON® FEP 100)) was purchased from Du Pont de Nemours Nederland B.V. The solvent, methyl isobutyl ketone (MIBK) was purchased from Acros Organics and methyl ethyl ketone (MEK) was purchased from Biosolve B.V. An adhesion promoting acrylic basecoat (experimental material XX/04901, a copolymer comprising of methyl methacrylate, lauryl methacrylate and 3-(trimethoxysilyl)propylmethacrylate), a commercial fluoropolymer, a non-biocidal marine fouling release coating (Intersleek® 1100SR), and polydimethylsiloxane (PDMS) were all supplied by Akzo Nobel N.V.

Preparation of TPE samples

Glass microscope slides were abraded (grit 150) and cleaned by sonication (in acetone, 15 min) and

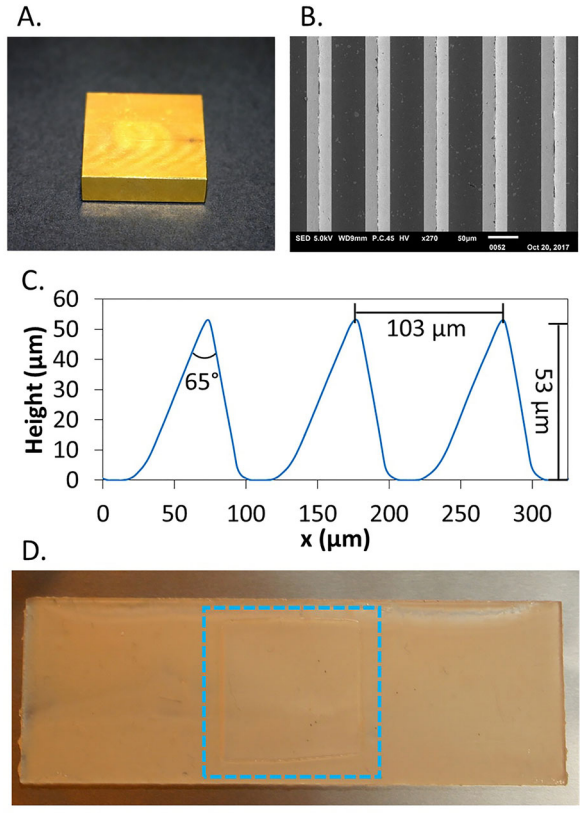

Figure 2. (A) Photograph of the master mould. (B) SEM image of the master mould surface. (C) Surface profile of the master mould (measured using a stylus profiler). (D) Photograph of an embossed TPE sample (dashed blue lines indicate the embossed area).

subsequently they were treated by UV-ozone in a photoreactor (Ultra Violet Products, PR100, 20 min). In order to aid adhesion, the substrates were first coated with an adhesion promoting acrylic basecoat using a doctor blade method with a slit height of 140 µm. An intermediate layer consisting of p(VDF-HFP) (30 wt%, dissolved in a 1:4 mixture of MEK and MIBK) was applied to aid adhesion between the AF finish coat and the basecoat. The AF coating was then applied, consisting of p(VDF-HFP) (30 wt%) and the lubricant PFPE (3 wt%, Solvay) dissolved in a 1:4 mixture of MEK and MIBK. Both of the TPE solutions were applied using a doctor blade method with a slit height of 630 µm. A schematic representation of the multilayer samples is shown in Figure 1.

A brass master mould (20 × 20 mm), which was micro-machined with a triangular diamond cutter, was made by the Equipment & Prototyping Centre of the

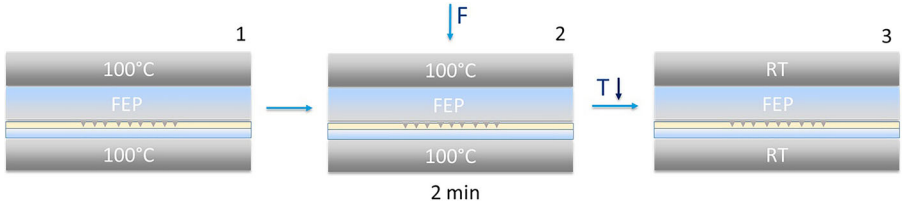

Figure 3. Schematic representation of embossing process: (1) Making a stack of the FEP mould and the TPE coated substrate and heating to 100 °C. (2) Applying a load on the stack for 2 min. (3) Cooling down to room temperature and removal of the FEP mould from the multilayer antifouling substrate.

Table 1. Name, description and the application process for the different coatings.

Name	Coating description	Application process
TPE smooth	Thermoplastic fluorinated co-polymer (flat)	Doctorblade coating
TPE with lubricant smooth	Thermoplastic fluorinated co-polymer with PFPE lubricant (flat)	Doctorblade coating
TPE with lubricant and riblets	Thermoplastic fluorinated co-polymer with PFPE lubricant (with micro-structured surface)	Doctorblade coating
Intersleek® 1100SR	Commercial fluoropolymer foul release coating	Brush
PDMS	Polydimethylsiloxane	Brush

University of Technology Eindhoven (Figure 2(A–C)). The trapezoidal grooves were based on the microstructures used in previous studies that showed drag reduction in comparison to flat surfaces (Bechert et al. 2000; Stenzel et al. 2011; Benschop et al. 2018). The direct use of the brass master resulted in adhesion issues and therefore the brass master was used to create an inverse (negative) copy of the microstructures in FEP. This FEP mould was created by mechanical embossing of the brass master in FEP sheets with a thickness of 10 mm. The master mould was placed on top of the FEP and the stack was heated to 270 °C in a mechanical embossing apparatus (Tribotrak, DACA). A load of 3 kg was applied on the stack for 2 min and subsequently the stack was cooled down to room temperature and the brass master was removed. The resulting negative FEP mould was used for thermal embossing of the positive hydrodynamic drag reduction structure in the TPE coating. As illustrated in Figure 3, the same embossing procedure was used at a temperature of 100 °C to create a micro-structured surface (25 × 25 mm) in the centre of the substrates (Figure 2(D)). An overview of the different materials and coating techniques is presented in Table 1.

Preparation of Intersleek® 1100SR and PDMS samples

Six replicate samples of Intersleek® 1100SR as a positive performance control coating and a pigmented polydimethylsiloxane (PDMS) elastomer as a negative or reference coating were applied to 76 mm × 25 mm × 2 mm PVC slides. All the PVC slides were cleaned by wiping with xylene before application of Intershield® 300 as a primer coat followed by Intersleek® 731 as a tie coat. The primer and tie coats were prepared in accordance with the manufacturer's instructions (www.international-marine.com) and applied by a small foam roller, the primer was cured for 24 h at 18 °C before the tie coat was applied followed by a further 24 h at 18 °C before the top coats of Intersleek®1100SR and PDMS were applied. The Intersleek® 1100SR was prepared in accordance with the manufacturer's instructions (www.international-marine.com) and applied using a synthetic brush. For the pigmented PDMS elastomer coating, DOW CORNING®3-0213 was used to which titanium dioxide (TIOXIDE TR92) and iron oxide (BAYFERROX BLACK 318 M) were added so as to match the grey colour of the Intersleek® 1100SR. The pigments were incorporated by mixing with a High Shear Disperser (HSD) mounted with an impeller blade. Before being applied by a synthetic brush a crosslinker (Wacker TES 40) and catalyst were added (TIB KAT 216) and hand mixed with a pallet knife.

Characterization

The brass master mould surface profile was measured using a stylus profiler (Dektak XT, Bruker) using a 2 µm radius stylus tip. The cross sections of TPE riblet surface structures were analysed using scanning electron microscopy (JSM-IT100, JEOL). To prepare the samples the TPE riblet surface structures were cooled in liquid nitrogen and cut with a razor blade in order to create cross sections. The cross sections were placed on aluminium stubs covered with carbon tape and sputter coated with a gold target at 60 mA for 30 s. These measurements were repeated in time

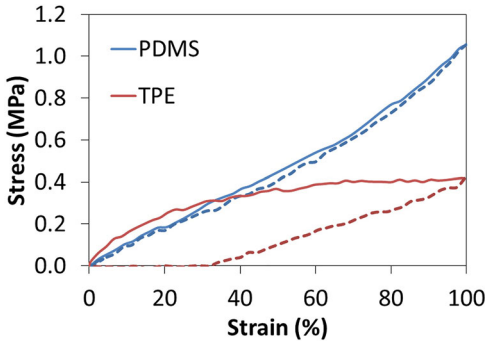

Figure 4. Stress–strain curves of PDMS and the thermoplastic elastomer (TPE). The solid lines shows stress under increasing strain, the dashed lines show stress under decreasing strain.

on multiple embossed samples, all kept under static laboratory condition (room temperature, in air, no illumination) to obtain the geometric data for a stability assay. Tensile tests were performed on a Lloyd EZ20 tensile tester (Lloyd Instruments) at room temperature using a 500 N load cell and a speed of 10 mm min^{-1}. Typically, a strip was stretched following a strain cycle starting at 0% strain, increasing to a strain of 100% and decreasing the strain again to 0%. Tensile bars were made from the TPE and a PDMS reference (Sylgard 184, Dow) according to ISO 527-2 (Type 5B, Gauge length 12 mm).

Biofilm growth and release testing

In order to evaluate the fouling-control performance, surfaces were tested in a biofilm culturing reactor, informally known as the 'slime farm' (Longyear 2014). The culture system is regularly inoculated by fresh biofilm, in this case, collected from non-toxic panels immersed (2–3 months) in the Raffles Marina in Singapore. Before the samples were transferred to the culturing reactor they were leached for three weeks in a 48 L tank. This tank was connected to a carbon filter with a turnover of 132 times h^{-1} running for 8 h day^{-1}. The biofilm culturing reactor consists of a recirculating artificial seawater system (temperature 22 ± 2 °C, salinity 33 ± 1 psu, pH 8.2 ± 0.2) into which a culture of microorganisms (mixed microalgae, including diatoms) was introduced. Under controlled hydrodynamic and environmental conditions marine biofilms are cultivated and subsequently grown on coated test surfaces. Five different coating types were assessed (Table 1). Samples were placed into the system for 75 days to allow biofilm growth on the surface (six glass or PVC slides for each coating type). After 75 days the samples were removed and tested for biofilm release in a variable-speed hydrodynamic flow-cell (Politis et al. 2009). The fouled microscope slides were installed in the flow cell and fully turbulent seawater was passed along the surfaces as described in the literature (Ventura et al. 2017; Benschop et al. 2018). The water velocity was incrementally increased from zero to 4.1 m s^{-1} (1.5, 2.1, 2.6, 3.1, 3.6 and 4.1 m s^{-1}), while remaining constant at each speed for 1 min. The slides were imaged with a digital camera (Powershot G1 X, Canon) before each speed increment and the amount of biofilm remaining on the surface as a percentage of the total area (% cover) was evaluated using image analysis software (Schneider et al. 2012). The percentage cover of biofilm was averaged across the six replicate slides and the mean percentage cover was compared between surfaces at each speed using ANOVA.

Results

Flat films without a microstructure were produced based on a thermoplastic elastomer (TPE) without lubricants. The mechanical performance of this material was compared with crosslinked PDMS. In Figure 4, it is shown that the Young's modulus of these materials was close to identical (PDMS: 1.4 ± 0.2 MPa; TPE: 2.0 ± 0.2 MPa) and the value for PDMS corresponds with previously reported moduli (Johnston et al. 2014). The PDMS sample exhibited a high degree of strain hardening and a high tensile strength, in contrast to the thermoplastic fluorinated copolymer. Moreover, the PDMS samples had a low tension set (<1%) and this in contrast to the TPE samples (32%). The low degree of strain hardening and the high tension set of the fluorinated copolymer is typical for thermoplastic and non-crosslinked systems and potentially has consequences for the properties of the coatings.

A polymeric master based on FEP was produced from a metallic original, as described in the materials and methods section. This FEP master had the inverse (negative) structure of the desired micro-structure for hydrodynamic drag reduction. Typically, the thermal embossing or imprinting of this microstructure was performed in the melt of the thermoplastic rubber and below the melting temperature of the polymeric (FEP) master and the sample was quenched to room temperature before release from the mould. The use of a perfluorinated master based on FEP was beneficial from a mould release point of view. The direct use of a metallic master resulted in strong adhesion between the master and the polymer which was circumvented by creating an intermediate FEP master. Micro-structures for hydrodynamic drag reduction were embossed in the coatings and typical examples of the original and the reproductions are shown

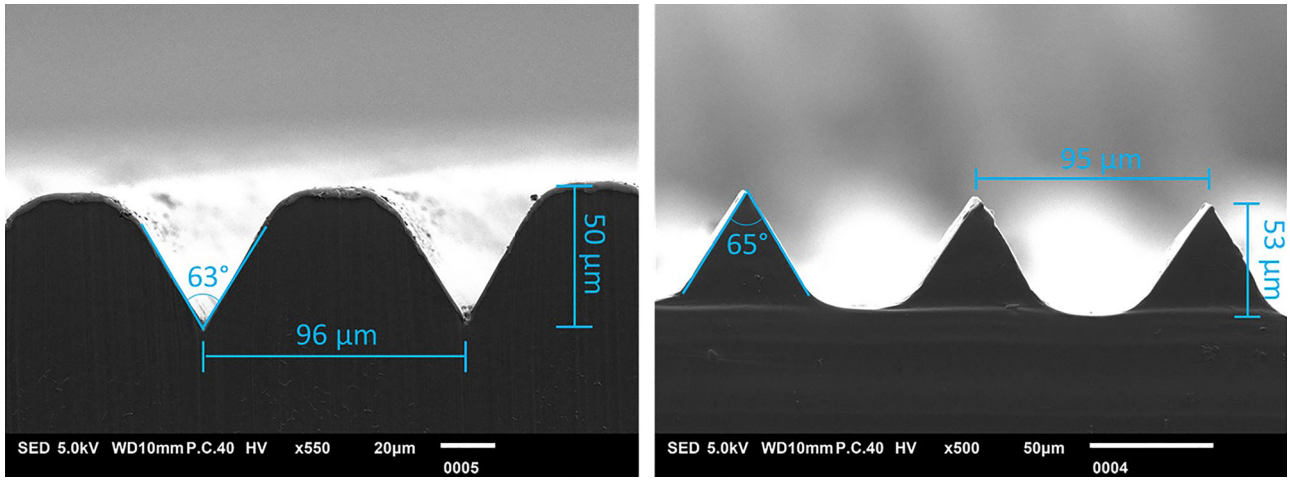

Figure 5. SEM images of the riblet surface in the FEP mould (left) and the TPE copy (right).

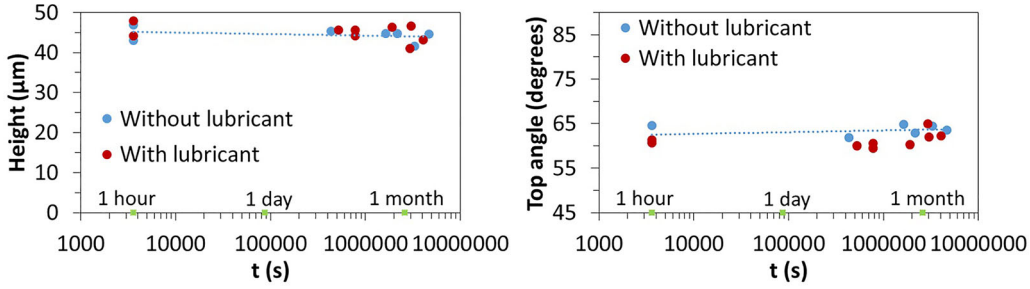

Figure 6. The height (left) and the top angle (right) of the riblet structures *vs* time for TPE coated samples with and without lubricant.

in Figure 5. It is shown that the microstructures were accurately reproduced in both the FEP master and in the AF coatings. A limited set of data was generated to explore the stability of the microstructures. In Figure 6, the height and top angle of the microstructures are plotted as a function of time. It is shown that the micro-structures did not change within the timescale of the experiments in TPE coatings with and without lubricants.

Before the samples were moved into the bio culturing reactor they were all leached as described in the materials and methods section. The biofilm growth on the samples at 0 flow rate was tested and significant variation was found (ANOVA, $F_{(4,24)} = 7.301$, $p = 0.0005$). The results are shown in Figure 7 (top row). It is shown that Intersleek® 1100SR, PDMS and the TPE without lubricant all had a high settlement. The addition of a lubricant to the TPE coatings reduced the settlement of biofilm quite significantly as is shown in the two most right columns in Figure 7. It seems that the settlement of marine biofilm on these coatings was low in comparison with all the reference samples, which is a rather unexpected result that is discussed in more detail later.

The adhesion strength of the marine biofilm was tested under dynamic conditions at an increasing water velocity to establish the influence of hydrodynamic shear rate. In Figure 7, it is shown that the commercial, non-biocidal coating (Intersleek® 1100SR) performed well, e.g. the initial settlement of marine biofilm was removed almost completely at moderate water velocity. The PDMS and TPE coating without lubricant, with a high initial settlement of marine biofilm, exhibited a poor performance with increasing hydrodynamic drag. The settlement of marine biofilm remained high up to high water velocity. The smooth TPE coating with lubricant outperformed the Intersleek® 1100SR coating at low water velocity, but had a higher final biofilm coverage. Whereas, the TPE coating with lubricant and riblets appeared to outperform all the other reference samples. The initial settlement in static conditions was already low and was rapidly removed from the materials at low water velocity.

The above-described observations were further quantified as described in the experimental section and the results are shown in Figure 8. In agreement with the results in Figure 7 it was found that, on

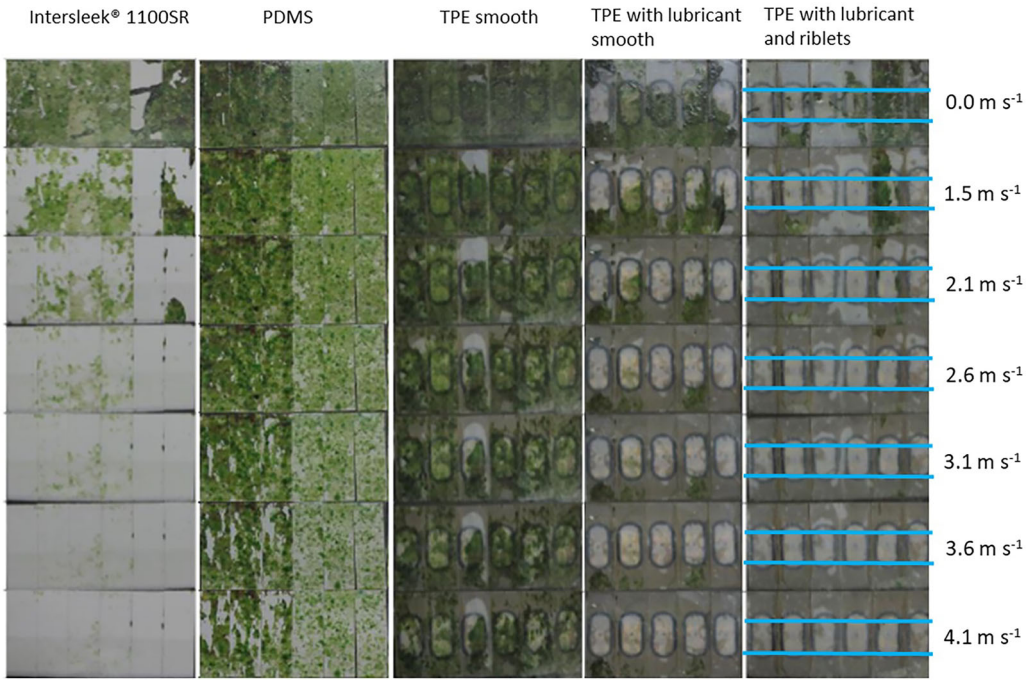

Figure 7. Photographs of the biofilm removal assays under increasing flow conditions (0–4.1 m s^{-1}). Only the embossed samples had a relief structure in the centre indicated by the blue lines (TPE with lubricant and riblets). Please note that the TPE samples are transparent, resulting in visibility of the clamping system holding the samples (the 5–6 rounded rectangles). The embossed structures are too small to see in the assay pictures.

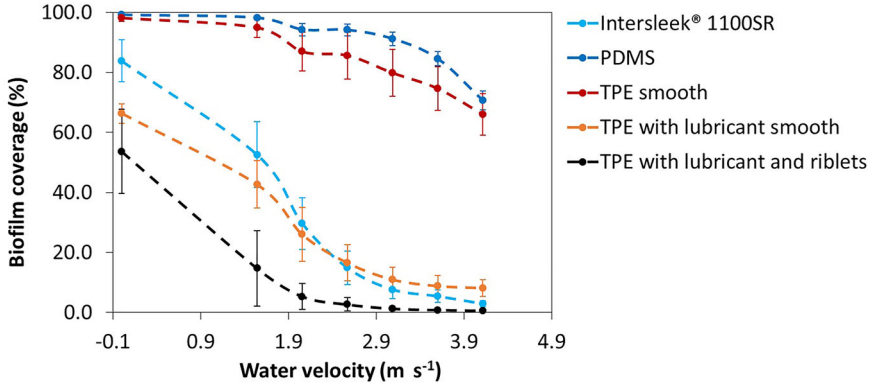

Figure 8. The mean percentage biofilm cover (±SE) as a function of water velocity. $N = 5$ for the TPE with lubricant smooth coating; for all other coatings $N = 6$.

average, the TPE coatings with lubricants outperformed all the reference samples in both static and low water velocity conditions. Moreover, it is also shown that microstructures for hydrodynamic drag reduction on average improved the performance even more, which is surprising in view of the previous literature (Benschop et al. 2018). However, when ANOVA was used to compare the biofilm coverage of the coatings, not all results proved significant. When comparing all coatings there is a significant difference at all water velocities. This was caused by the large difference between PDMS and TPE compared with Intersleek® 1100SR and the TPE coatings with lubricant, for example at 2.1 m s^{-1} (ANOVA, $F_{(4,24)} = 38.614$, $p < 0.0005$). When the TPE coatings with lubricant were compared with Intersleek® 1100SR significant variation was only found at the final water velocity (ANOVA, $F_{(2,14)} = 5.830$, $p = 0.014$). Moreover, this variation was caused by a significant effect of the riblets. This becomes clear when comparing the TPE coatings with lubricant at the final water velocity (ANOVA, $F_{(1,9)} = 8.433$, $p = 0.017$). The results in Figure 8 were obtained using images of the whole sample. However, the samples with riblets were only partially embossed (see Figure 7). As a consequence, the real fouling release (FR) properties are probably better than the results presented in Figure 8.

Discussion

Conventional non-biocidal FR coatings for a marine environment are usually based on crosslinked fluoropolymers or crosslinked PDMS-like materials with or without lubricants (Lejars et al. 2012). In specific cases, surface relief structures are employed to enhance the FR properties or to reduce hydrodynamic drag (Yao et al. 2014; Benschop et al. 2018). Unfortunately, the material cost of such coatings is quite high and the generation of surface relief structures is laborious and difficult to scale-up due to the crosslinked nature of these coatings. Processes to generate such surface relief structures have been developed but involve complex and costly mask exposures, etching procedures and/or dedicated equipment for simultaneous ultra-violet light curing and surface structuring (Stenzel et al. 2010; Stenzel et al. 2011; Kordy 2015; Kommeren et al. 2016; Kommeren et al. 2019).

Thermoplastic (and non-crosslinked) polymers are often preferred from a material and processing cost point of view which is often related to their lower cost and ease of processing. Thermoplastic materials do not require complex curing cycles and surface relief structures can be generated with high speed thermal processes such as imprinting/embossing, calendaring and/or injection moulding. Therefore, it was decided to use these thermoplastic materials as the materials of choice for this study.

A few critical remarks are appropriate with respect to the results presented above. Firstly, the transfer of the samples from the recirculating artificial seawater system to the controlled hydrodynamic shear environment in some cases introduced a loss in fouling which was induced by the flow of water upon transfer. Consequently, the data points in Figure 8 at zero water velocity might have experienced a (very low) water velocity and should be slightly shifted to a little bit above zero water velocity. On the other hand, this hardly changes the main observations in this study and this was therefore ignored. Secondly, this study was limited to a single thermoplastic elastomer and a single lubricant which was added in a single weight fraction (10 wt%). A further optimisation of the coatings with respect to the chemical structure of the TPE, lubricant and weight fractions would potentially result in further improvements of these coatings in marine AF. Thirdly, a limited set of data was presented concerning the long term stability of the coatings and more extensive studies need to be performed on large scale vessels to further establish their practical applications and limitations. Fourthly, the samples had only been partially embossed which could result in edge effects on the boundary of the embossed area. However, when looking closely at the boundary region in Figure 7 no such effect is seen. The release of biofilm seems to be similarly spread when compared to the reference samples. Finally, the TPE with lubricant and a micro-structure on average exhibited an improved performance in comparison to their flat and lubricant free counterparts. This rather unexpected result seems to contradict another study which was performed on modified Intersleek® 1100SR (Benschop et al. 2018) in which hardly any influence of the hydrodynamic shear reducing structures was observed. At present, the origin of this phenomenon is obscure and therefore no speculation has been made on this. Despite the rather obvious limitations described above, it is believed that the results of this study are relevant for practical applications in a marine environment.

Conclusions

Thermoplastic elastomers (TPEs) were used as AF coatings in a marine environment and it was found that these showed a promising performance both in static and dynamic conditions. Moreover, the FR performance is at least comparable to Intersleek® 1100SR and more experiments are necessary to strengthen the significance of the trends seen in the biofilm coverage means, in particular with regard to the potential beneficial effect of the riblets on the AF performance. It is anticipated that these coatings have significant cost advantages compared to their crosslinked counterparts and are potentially useful in a marine environment, especially in hydrodynamic shear applications such as marine vessels.

Acknowledgements

The authors would like to thank J.J.B. van der Tol for his help during the manufacturing of the TPE samples.

Disclosure statement

No potential conflict of interest was reported by the author(s).

Funding

This work was supported by the European Union Seventh Framework Programme in the SEAFRONT project under Grant [614034].

ORCID

Tom Bus http://orcid.org/0000-0001-6325-5922

References

Bechert DW, Bruse M, Hage W. 2000. Experiments with three-dimensional riblets as an idealized model of shark skin. Exp Fluids. 28:403–412. doi:10.1007/s003480050400

Benschop HOG, Guerin AJ, Brinkmann A, Dale ML, Finnie AA, Breugem WP, Clare AS, Stübing D, Price C, Reynolds KJ. 2018. Drag-reducing riblets with fouling-release properties: development and testing. Biofouling. 34:532–544. doi:10.1080/08927014.2018.1469747

Boggs EM, Aizenberg J, Epstein AK, Wong T-S, Belisle RA. 2012. Liquid-infused structured surfaces with exceptional anti-biofouling performance. Proc Natl Acad Sci USA. 109:13182–13187. doi:10.1073/pnas.1201973109

Dafforn KA, Lewis JA, Johnston EL. 2011. Antifouling strategies: history and regulation, ecological impacts and mitigation. Mar Pollut Bull. 62:453–465. doi:10.1016/j.marpolbul.2011.01.012

Deshpande A, Smith GWG, Smith AJ. 2015. Biofouling of surgical power tools during routine use. J Hosp Infect. 90:179–185. doi:10.1016/j.jhin.2015.03.006

Harding JL, Reynolds MM. 2014. Combating medical device fouling. Trends Biotechnol. 32:140–146. doi:10.1016/j.tibtech.2013.12.004

He W, Liu P, Zhang J, Yao X. 2018. Emerging applications of bioinspired slippery surfaces in biomedical fields. Chem Eur J. 24:14864–14877. doi:10.1002/chem.201801368

Jiang S, Li Y, Ladewig BP. 2017. A review of reverse osmosis membrane fouling and control strategies. Sci Total Environ. 595:567–583. doi:10.1016/j.scitotenv.2017.03.235

Johnston ID, McCluskey DK, Tan CKL, Tracey MC. 2014. Mechanical characterization of bulk Sylgard 184 for microfluidics and microengineering. J Micromech Microeng. 24:035017. doi:10.1088/0960-1317/24/3/035017

Kommeren S, Guerin AJ, Dale ML, Ferguson J, Lyall G, Reynolds KJ, Clare AC, Bastiaansen CWM, Sullivan T. 2019. Antifouling and fouling-release performance of photo-embossed fluorogel elastomers. J Mar Sci Eng. 7:419. doi:10.3390/jmse7110419

Kommeren S, Sullivan T, Bastiaansen C. 2016. Tunable surface topography in fluoropolymers using photo-embossing. RSC Adv. 6:69117–69123. doi:10.1039/C6RA13801B

Konstantinou IK, Albanis TA. 2004. Worldwide occurrence and effects of antifouling paint booster biocides in the aquatic environment: a review. Environ Int. 30:235–248. doi:10.1016/S0160-4120(03)00176-4

Kordy H. 2015. Process abilities of the riblet-coating process with dual-cure lacquers. CIRP J Manuf Sci Technol. 11:1–9. doi:10.1016/j.cirpj.2015.08.003

Lejars M, Margaillan A, Bressy C. 2012. Fouling release coatings: a nontoxic alternative to biocidal antifouling coatings. Chem Rev. 112:4347–4390. doi:10.1021/cr200350v

Longyear J. 2014. Laboratory experiments and cultures. Section 2. In: Dobretsov S, Williams DN, Thomason JC, editors. Biofouling methods. Chichester (UK): John Wiley & Sons, Ltd.; p. 214–219.

Miserez A, Amini S, Sutanto CN, Ahanotu O, Petrone L, Kolle S, Sunny S, Aizenberg J, Weaver JC, Vogel N, et al. 2017. Preventing mussel adhesion using lubricant-infused materials. Science. 357:668–673. doi:10.1126/science.aai8977

Nurioglu AG, Esteves ACC, De With G. 2015. Non-toxic, non-biocide-release antifouling coatings based on molecular structure design for marine applications. J Mater Chem B. 3:6547–6570. doi:10.1039/C5TB00232J

Politis G, Atlar M, Downie M. 2009. AMT'09. Design of a turbulent channel flow facility for antifouling coating research. Proceedings of the 1st Advanced Model Measurement Technology for the EU Maritime Industry; Sep 1–2; Nantes, France: Ecole Centrale de Nantes. p. 252–265.

Schneider CA, Rasband WS, Eliceiri KW. 2012. NIH Image to ImageJ: 25 years of image analysis. Nat Methods. 9:671–675. doi:10.1038/nmeth.2089

Schultz MP. 2007. Effects of coating roughness and biofouling on ship resistance and powering. Biofouling. 23:331–341. doi:10.1080/08927010701461974

Schultz MP, Bendick JA, Holm ER, Hertel WM. 2011. Economic impact of biofouling on a naval surface ship. Biofouling. 27:87–98. doi:10.1080/08927014.2010.542809

Stenzel V, Kaune M, Da Silva Branco Cheta MR. 2010. Fraunhofer-Gesellschaft zur Forderung der Angewandten Forschung E.V. 2010 Jun 15. Tool for generating micro-structured surfaces. US. 7,736,570 B2.

Stenzel V, Wilke Y, Hage W. 2011. Drag-reducing paints for the reduction of fuel consumption in aviation and shipping. Prog Org Coat. 70:224–229. doi:10.1016/j.porgcoat.2010.09.026

Thomas KV, Brooks S. 2010. The environmental fate and effects of antifouling paint biocides. Biofouling. 26:73–88. doi:10.1080/08927010903216564

Ventura C, Guerin AJ, El-Zubir O, Ruiz-Sanchez AJ, Dixon LI, Reynolds KJ, Dale ML, Ferguson J, Houlton A, Horrocks BR, et al. 2017. Marine antifouling performance of polymer coatings incorporating zwitterions. Biofouling. 33:892–903. doi:10.1080/08927014.2017.1383983

Wong TS, Kang SH, Tang SKY, Smythe EJ, Hatton BD, Grinthal A, Aizenberg J. 2011. Bioinspired self-repairing slippery surfaces with pressure-stable omniphobicity. Nature. 477:443–447. doi:10.1038/nature10447

Xiao L, Li J, Mieszkin S, Di Fino A, Clare AS, Callow ME, Callow JA, Grunze M, Rosenhahn A, Levkin PA. 2013. Slippery liquid-infused porous surfaces showing marine antibiofouling properties. ACS Appl Mater Interfaces. 5:10074–10080. doi:10.1021/am402635p

Yao X, Dunn SS, Kim P, Duffy M, Alvarenga J, Aizenberg J. 2014. Fluorogel elastomers with tunable transparency, elasticity, shape-memory, and antifouling properties. Angew Chem Int Ed. 53:4418–4422. doi:10.1002/anie.201310385